

**Electronic Supplementary Information**

**S-nitrosated Biodegradable Polymers for Biomedical Applications: Synthesis,  
Characterization and Impact of Thiol Structure on the Physicochemical Properties**

Vinod B. Damodaran,<sup>a</sup> Jessica M. Joslin,<sup>a</sup> Kathryn A. Wold,<sup>b</sup> Sarah M. Lantvit<sup>a</sup> and  
Melissa M. Reynolds<sup>ab\*</sup>

<sup>a</sup>Department of Chemistry, Colorado State University, Fort Collins, CO 80523, USA.

<sup>b</sup>School of Biomedical Engineering, Colorado State University, Fort Collins, CO 80523,  
USA.

\*Corresponding Author:

E-mail: melissa.reynolds@colostate.edu

Tel: +1 970 491 3775

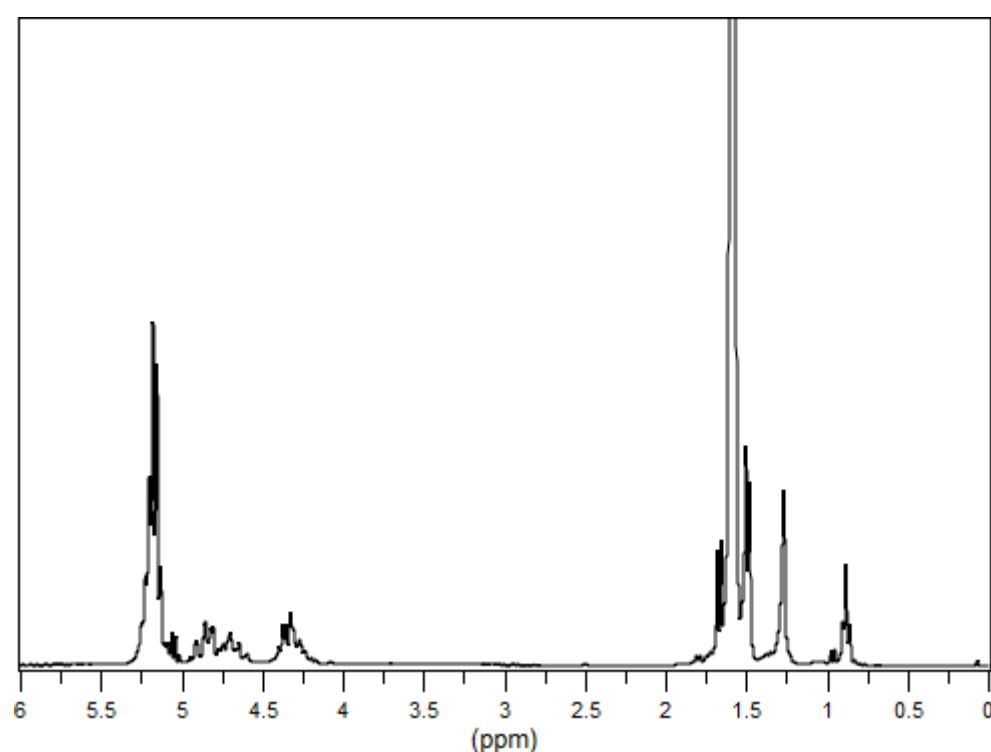
Contents	Page No.
S1. $^1\text{H}$ NMR characterization.....	S4-S7
S1a. PLGH $^1\text{H}$ NMR (Fig. S1).....	S4
S1b. PLGH-cysteamine $^1\text{H}$ NMR (Fig. S2).....	S5
S1c. PLGH-cysteine $^1\text{H}$ NMR (Fig. S3).....	S6
S1d. PLGH-homocysteine $^1\text{H}$ NMR (Fig. S4).....	S7
S2. IR characterization (Fig. S5).....	S8-S9
S3. Elemental analysis (Table S1).....	S10
S4. Thermal analysis.....	S11-S16
S4a. Thermal gravimetric analysis (TGA).....	S11-S13
i. Fig. S6: TGA thermogram of PLGH.....	S11
ii. Fig. S7: TGA thermograms of PLGH-thiol derivatives.....	S12-S13
S4b. Differential scanning calorimetry (DSC).....	S14-S16
i. Fig. S8: DSC thermogram of PLGH.....	S14
ii. Fig. S9: DSC thermograms of PLGH-thiol derivatives.....	S15-S16
S5. SAXS analysis (Fig. S10).....	S17
S6. Contact angle (Fig. S11).....	S18
S7. Cytotoxicity.....	S19
i. Table S2: Reactivity grades for material cytotoxicity.....	S19
S8. S-nitrosation reaction kinetics.....	S20-S21
i. Fig. S12: UV spectrum of PLGH-cysteamine w/ <i>t</i> -butyl nitrite.....	S20
ii. Fig. S13: <i>S</i> -nitrosation kinetics of PLGH-cysteamine.....	S20
iii. Fig. S14: <i>S</i> -nitrosation kinetics of PLGH-cysteine.....	S21
iv. Fig. S15: <i>S</i> -nitrosation kinetics of PLGH-homocysteine.....	S21

S9. Molar extinction coefficient determination.....	S22-S25
i. Fig. S16: Absorbance vs. polymer concentration plots.....	S22
ii. Fig. S17: UV spectra before/after NO release.....	S24
iii. Table S3: NO recovery and absorption properties of polymers.....	S25
S10. NO releasing kinetics.....	S26
i. Fig. S18: NO release profile for PLGH-cysteine over 70 h.....	S26
References.....	S27

**S1.  $^1\text{H}$  NMR characterization**

**S1a. PLGH**

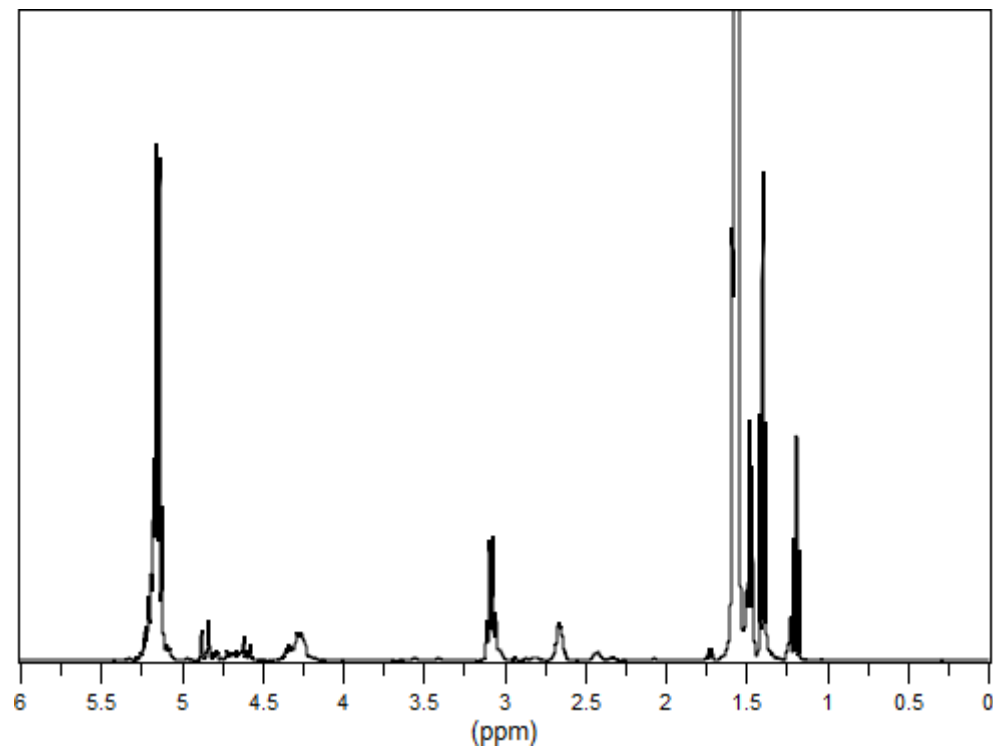
$^1\text{H}$  NMR ( $\text{CDCl}_3$ ):  $\delta$  5.17 (m, -O-CH(CH<sub>3</sub>)-CO-), 1.59 (d, -O-CH(CH<sub>3</sub>)-CO-), 4.58 – 4.90 (m, -O-CH-CO-), 4.18 – 4.40 (m, -O-CH<sub>2</sub>-C-) and 1.27 (s, -CH<sub>2</sub>-C(CH<sub>3</sub>)-).



**Fig. S1**  $^1\text{H}$  NMR of PLGH in  $\text{CDCl}_3$ .

**S1b.** PLGH-cysteamine (**1a**)

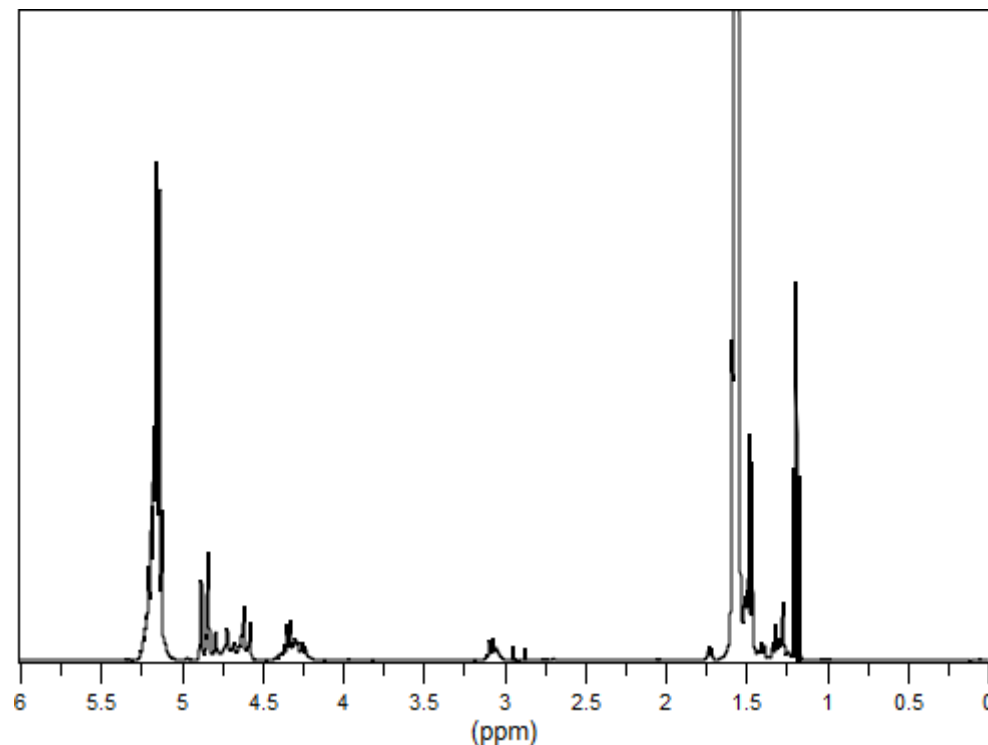
$^1\text{H}$  NMR ( $\text{CDCl}_3$ ):  $\delta$  3.09 (m, -NH-CH<sub>2</sub>-CH<sub>2</sub>-) and 2.64 (m, -NH-CH<sub>2</sub>-CH<sub>2</sub>-).



**Fig. S2**  $^1\text{H}$  NMR of PLGH-cysteamine (**1a**) in  $\text{CDCl}_3$ .

**S1c.** PLGH-cysteine (**1b**)

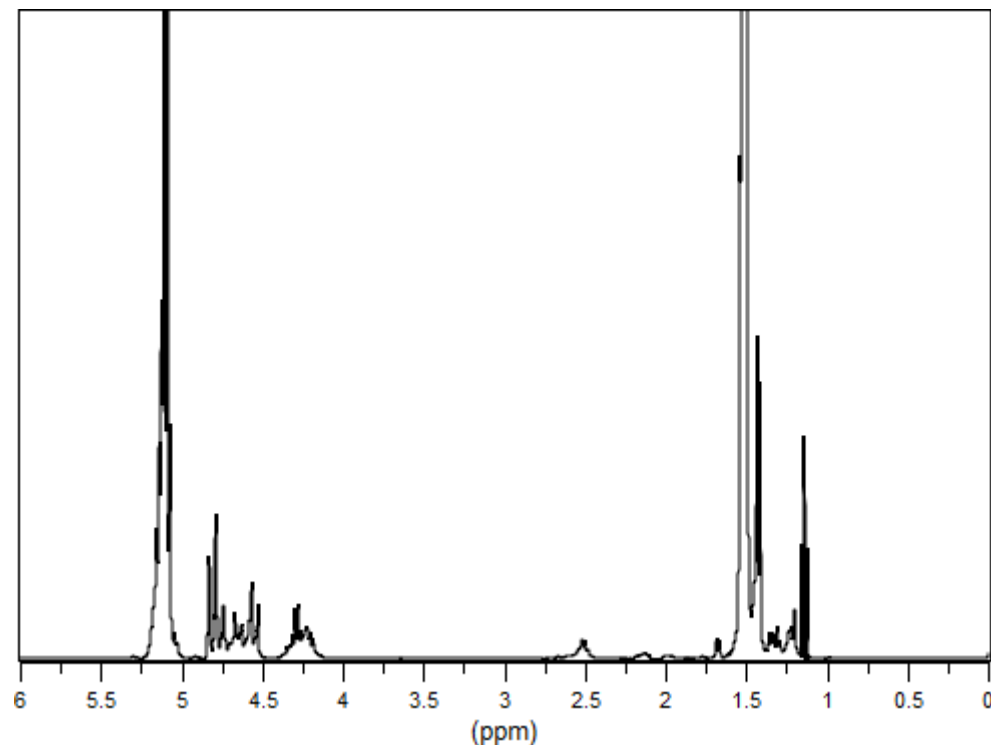
$^1\text{H}$  NMR ( $\text{CDCl}_3$ ):  $\delta$  3.07 (m, -NH-CH<sub>2</sub>-SH).



**Fig. S3**  $^1\text{H}$  NMR of PLGH-cysteine (**1b**) in  $\text{CDCl}_3$ .

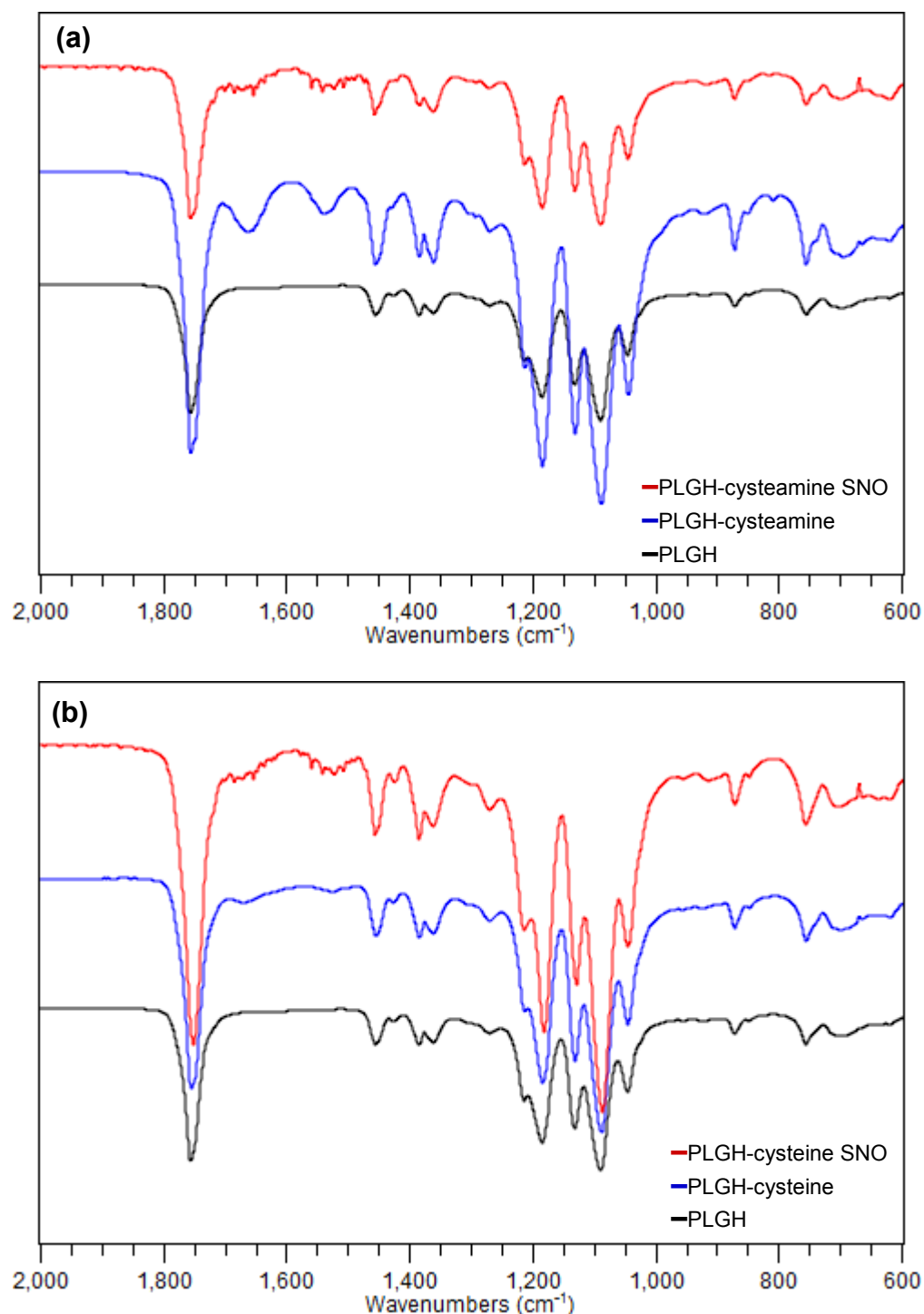
**S1d.** PLGH-homocysteine (**1c**)

$^1\text{H}$  NMR ( $\text{CDCl}_3$ ):  $\delta$  2.12 (m, -NH-CH<sub>2</sub>-CH<sub>2</sub>-) and 2.51 (m, -NH-CH<sub>2</sub>-CH<sub>2</sub>-).



**Fig. S4**  $^1\text{H}$  NMR of PLGH-homocysteine (**1c**) in  $\text{CDCl}_3$ .

**S2. IR characterization**



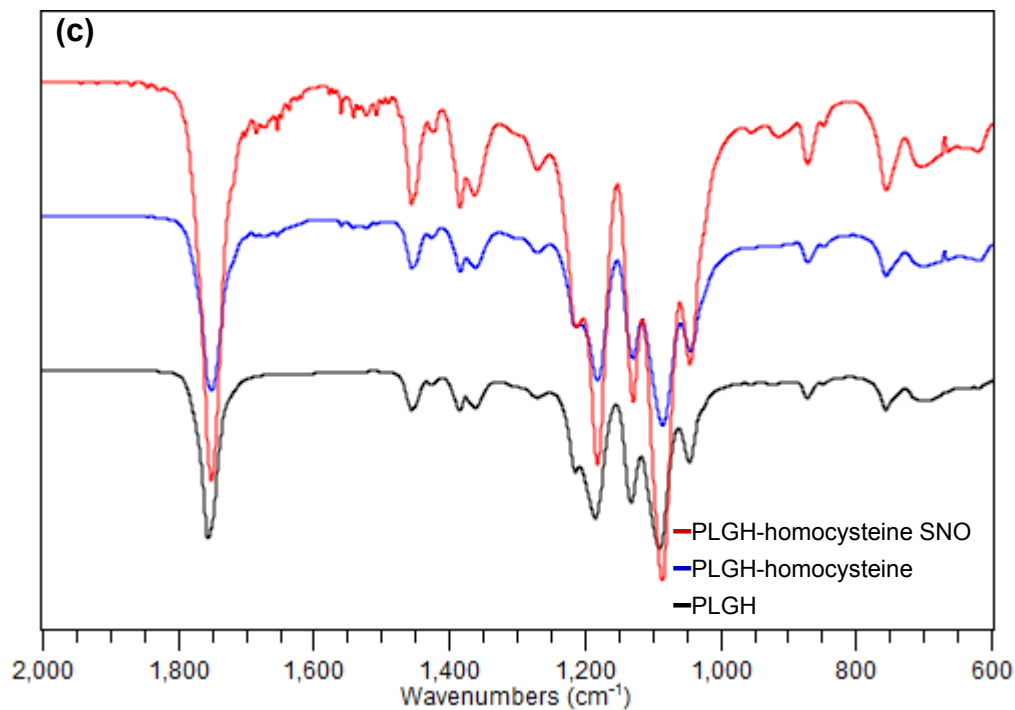


**Fig. S5** FTIR spectra of PLGH and the corresponding (a) cysteamine, (b) cysteine and (c) homocysteine derivatives, before and after S-nitrosation.

### S3. Elemental analysis

**Table S1** Elemental composition of polymers

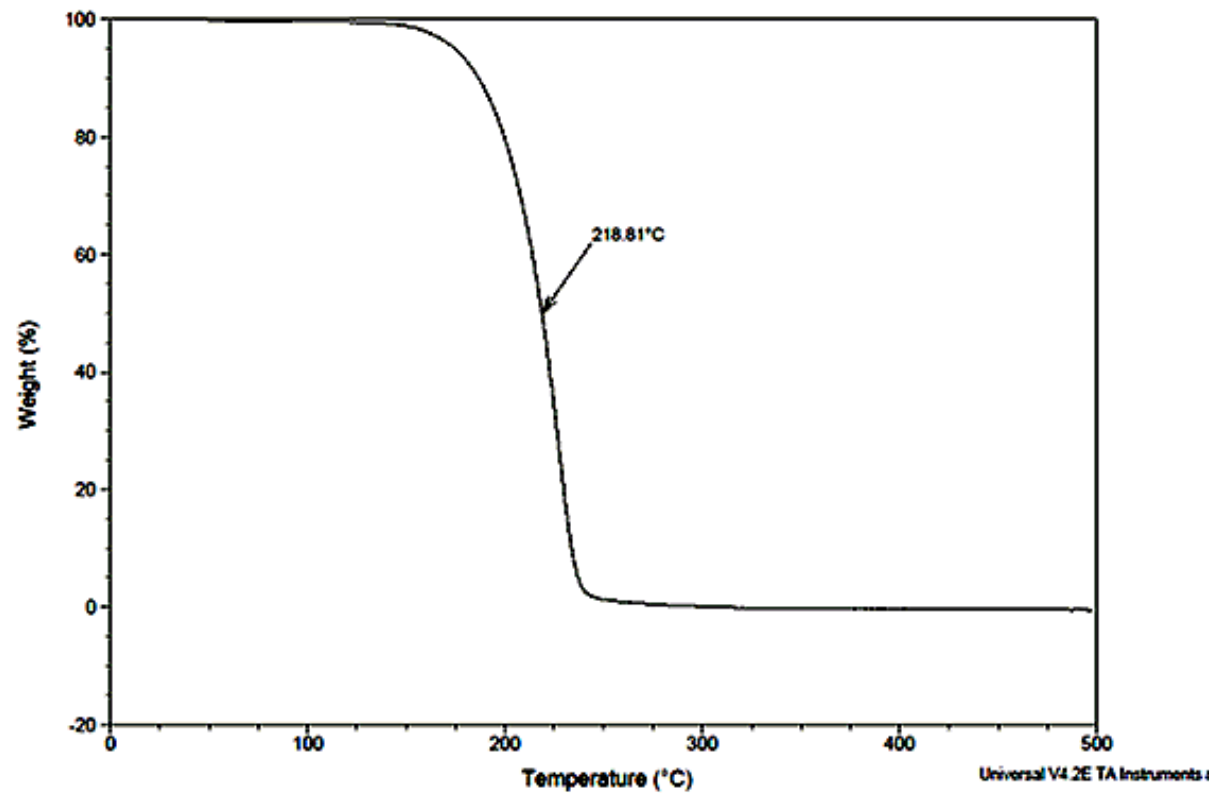
Sample	Calculated*				Analyzed			
	% H	% C	% N	% S	% H	% C	% N	% S
PLGH	5.31	48.47	--	--	5.45	48.67	--	--
PLGH-cysteamine	5.49	47.76	1.76	4.01	6.03	47.77	2.39	3.50
PLGH-cysteamine SNO	5.42	47.08	2.41	3.10	5.90	47.96	1.69	2.35
PLGH-cysteine	5.31	47.67	0.66	1.16	5.53	48.08	0.86	1.39
PLGH-cysteine SNO	5.27	47.46	0.92	1.15	5.55	47.90	0.98	1.29
PLGH-homocysteine	5.27	48.32	0.49	1.10	5.67	48.93	0.66	1.12
PLGH-homocysteine SNO	5.23	48.11	0.58	0.95	5.55	48.46	0.72	1.05

\*Calculated based on NMR composition for parent and thiolated polymers and percentage *S*-nitrosation for *S*-nitrosated polymers

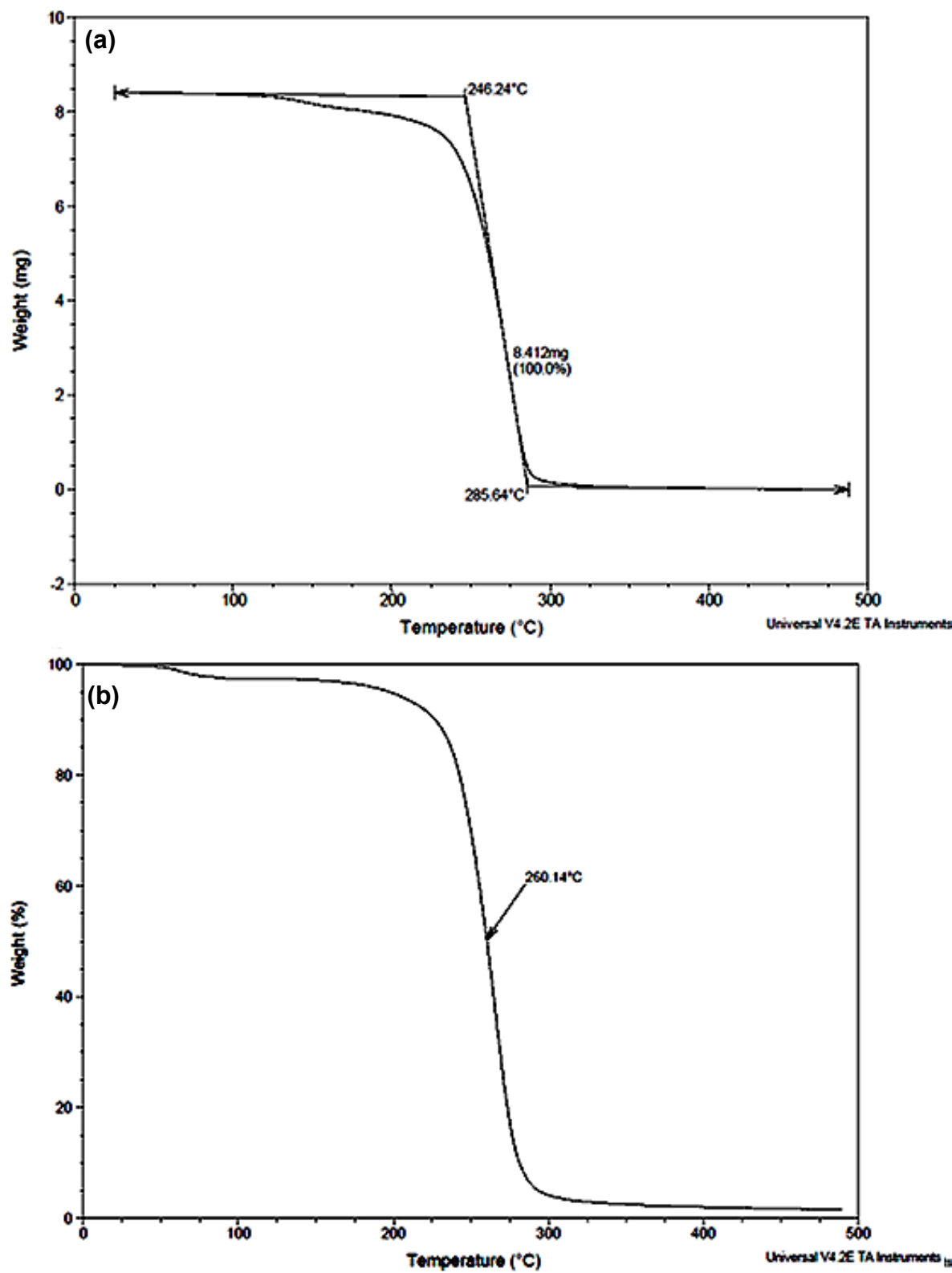
## S4. Thermal analysis

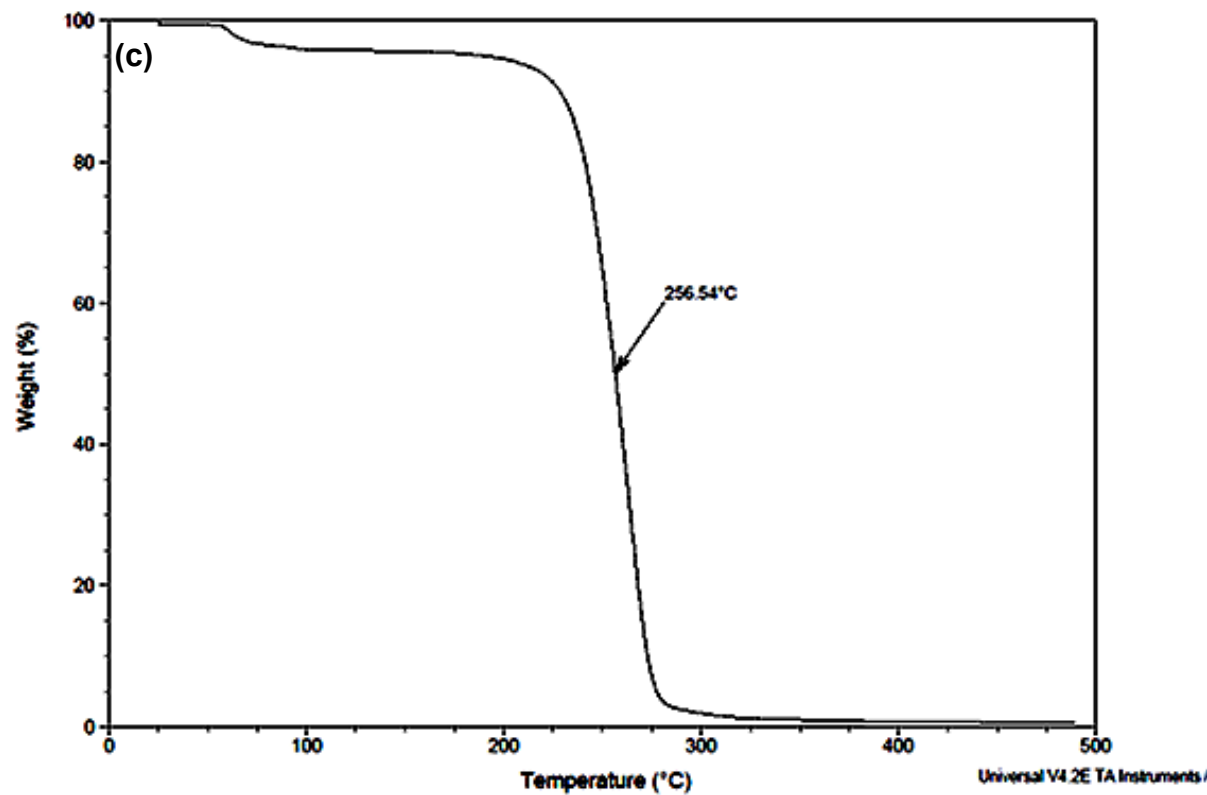
### S4a. Thermal gravimetric analysis

(TGA)



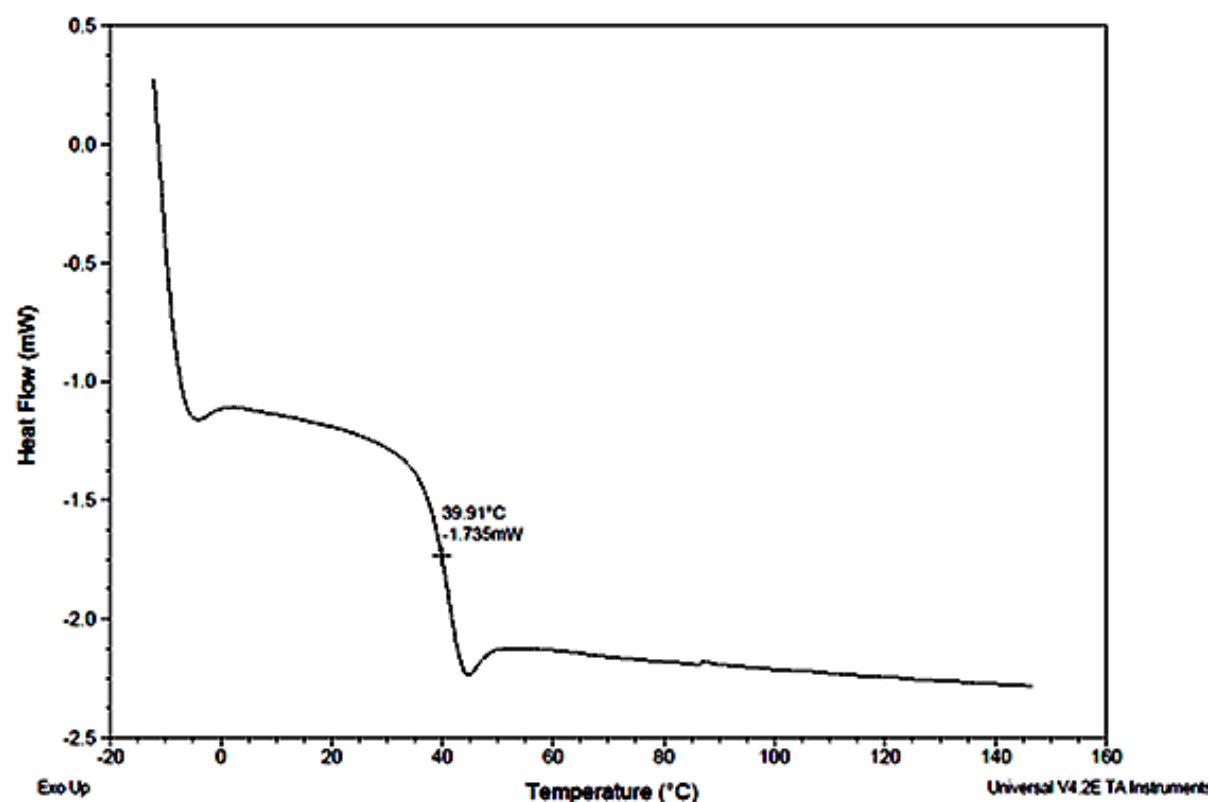
**Fig. S6** A representative TGA thermogram of PLGH.



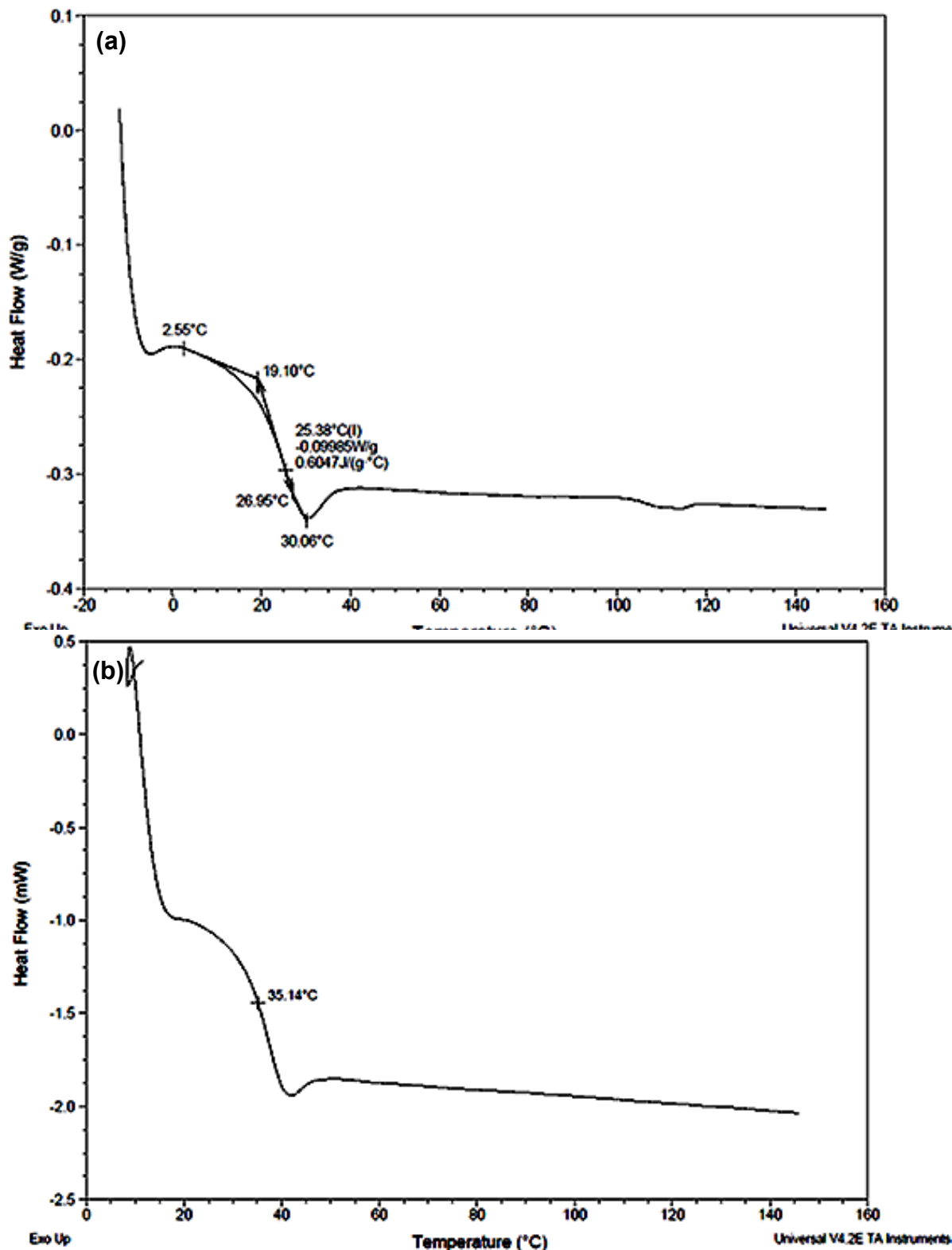


**Fig. S7** Representative TGA thermograms of PLGH modified with (a) cysteamine (**1a**), (b) cysteine (**1b**) and (c) homocysteine (**1c**).

**S4b. Differential scanning calorimetry (DSC)**



**Fig. S8** A representative DSC thermogram of PLGH.



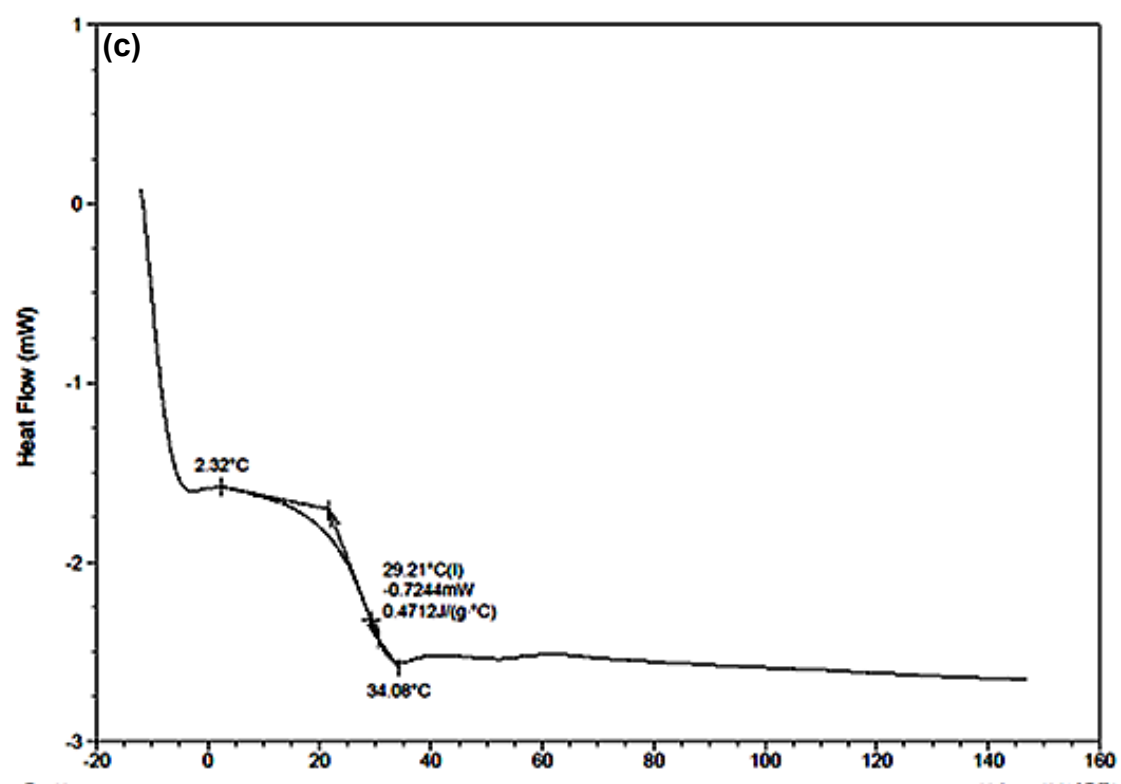


**Fig. S9** Representative DSC thermograms of PLGH modified with (a) cysteamine (**1a**), (b) cysteine (**1b**) and (c) homocysteine (**1c**).

**S5. Small angle X-ray scattering (SAXS) analysis**

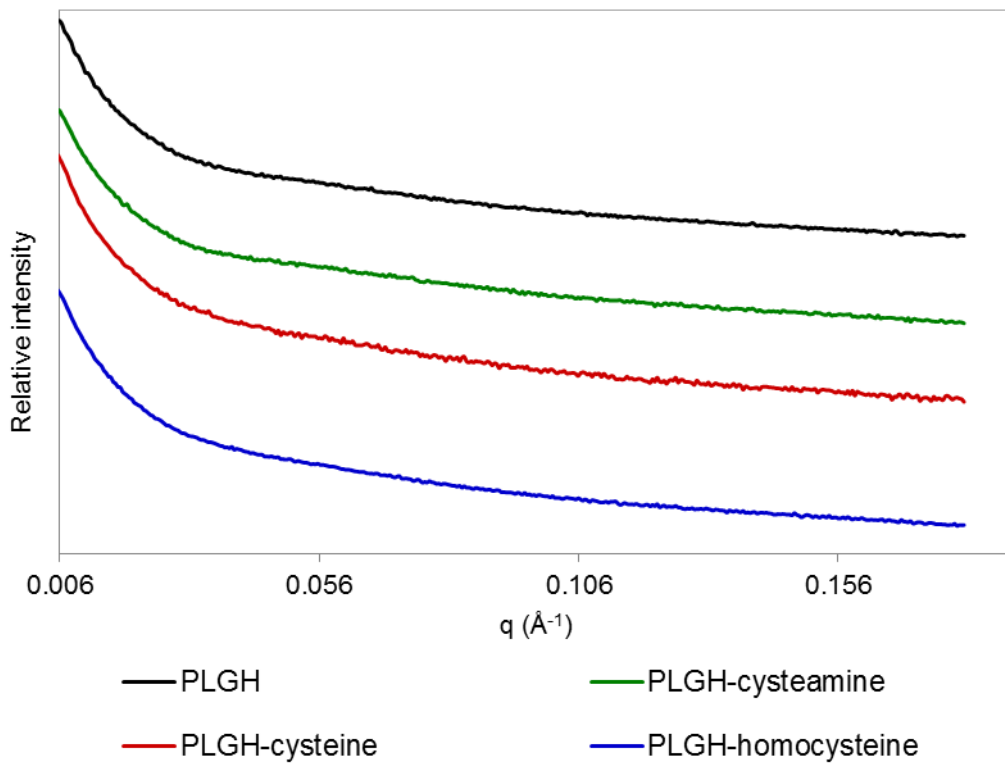


**Fig. S10** SAXS intensity profiles of various polymers at 25 °C indicate amorphous structures.

**S6. Contact angle**

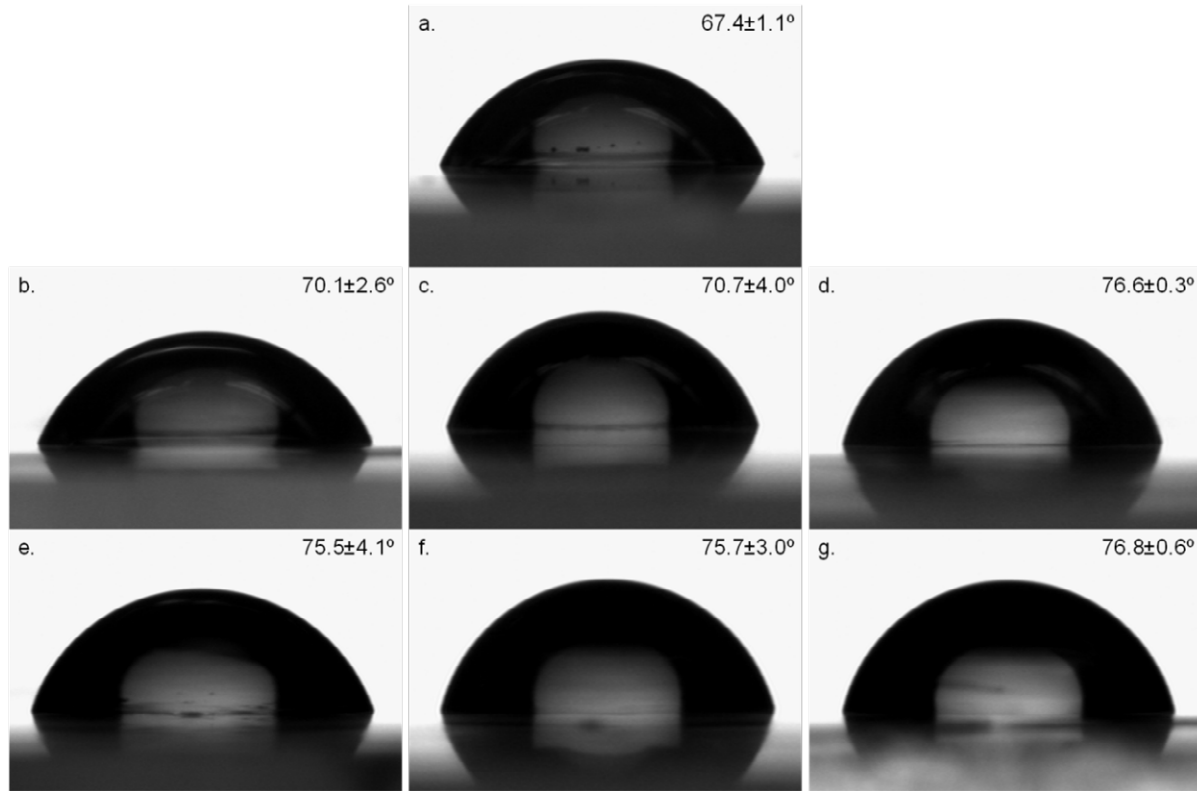


**Fig. S11** Contact angles for PLGH and modified PLGH polymers: (a) PLGH, (b) PLGH-cysteamine (**1a**), (c) PLGH-cysteine (**1b**), (d) PLGH-homocysteine (**1c**), (e) *S*-nitrosated PLGH-cysteamine (**2a**), (f) *S*-nitrosated PLGH-cysteine (**2b**), and (g) *S*-nitrosated PLGH-homocysteine (**2c**).

### S7. Cytotoxicity – Reactivity grade summary

Cytotoxicity of thiolated polymer samples was analyzed at NAMSA (Northwood, OH, USA) following the method given in Section 2.5. The results were evaluated using Table S2.

**Table S2** Reactivity grades for material cytotoxicity

<b>Grade</b>	<b>Reactivity</b>	<b>Conditions of Cell Cultures</b>
0	None	Discrete intracytoplasmic granules, no cell lysis, no reduction of cell growth.
1	Slight	Not more than 20% of the cells are round, loosely attached and without intracytoplasmic granules, or show changes in morphology; occasional lysed cells are present; only slight growth inhibition observed.
2	Mild	Not more than 50% of the cells are round, void of intracytoplasmic granules; no extensive cell lysis; not more than 50% growth inhibition observed.
3	Moderate	Not more than 70% of the cell layers contain rounded cells or are lysed; cell layers not completely destroyed, but more than 50% growth inhibition observed.
4	Severe	Nearly complete or complete destruction of the cell layers.

### S8. S-nitrosation reaction kinetics

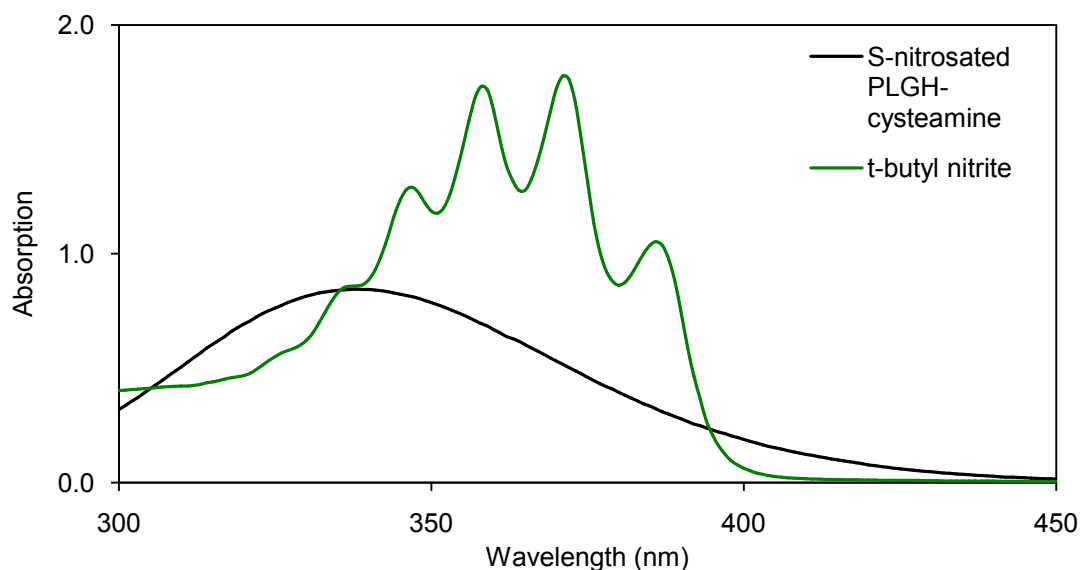


**Fig. S12** A representative UV absorption profile of *S*-nitrosated PLGH-cysteamine (**2a**) showing complete removal of excess *t*-butyl nitrite from the product.

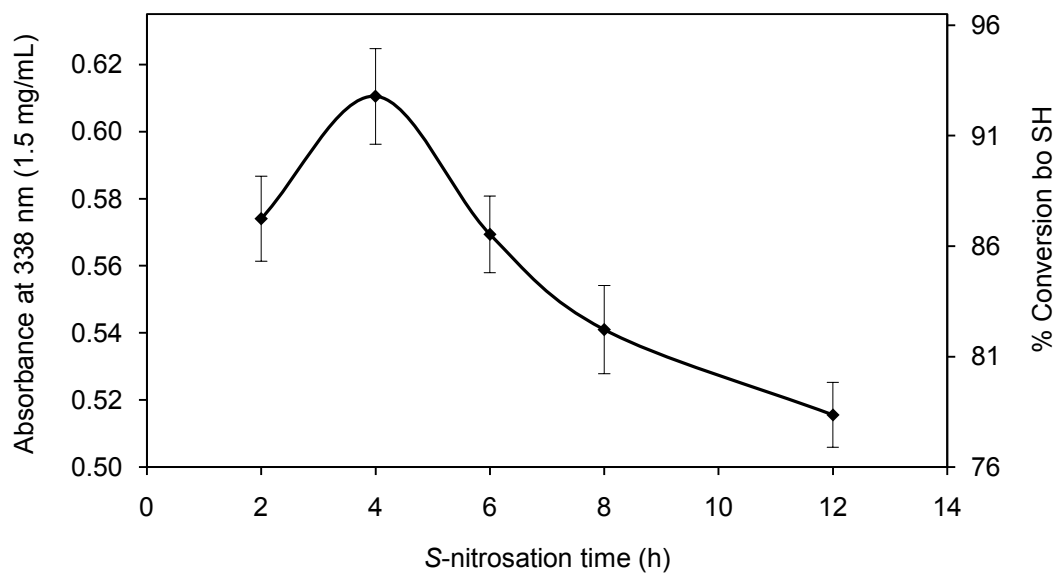


**Fig. S13** *S*-nitrosation reaction kinetics of PLGH-cysteamine (**2a**), as modified from our previous publication<sup>1</sup> to include % conversion based on SH values.

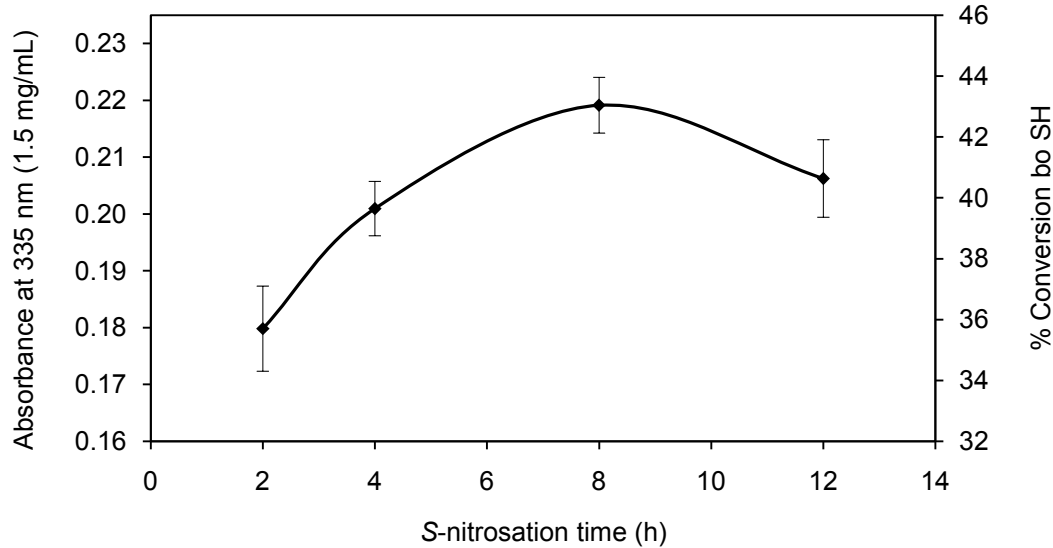


**Fig. S14** S-nitrosation reaction kinetics of PLGH-cysteine (**2b**).

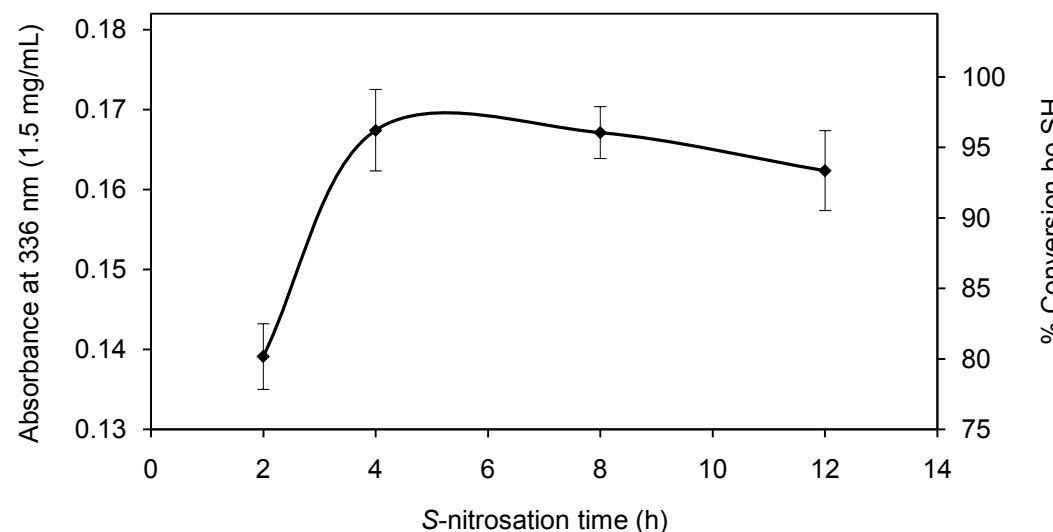


**Fig. S15** S-nitrosation reaction kinetics of PLGH-homocysteine (**2c**).

## S9. Molar extinction coefficient determination

To determine a molar extinction coefficient value ( $\epsilon_{\max}$ ) associated with the  $\lambda_{\max}$  of each *S*-nitrosated PLGH derivative, the following was performed. A series of freshly *S*-nitrosated polymer solutions were prepared in a concentration range of 0-1.75, 0-4, and 0-10 mg polymer mL<sup>-1</sup> (2 methanol: 1 dichloromethane solvent) for cysteamine (**2a**), cysteine (**2b**), and homocysteine (**2c**) derivatives, respectively. The calibration curves shown in Fig. S16 indicate the absorption values at the  $\lambda_{\max}$  as a function of polymer concentration for each derivative.

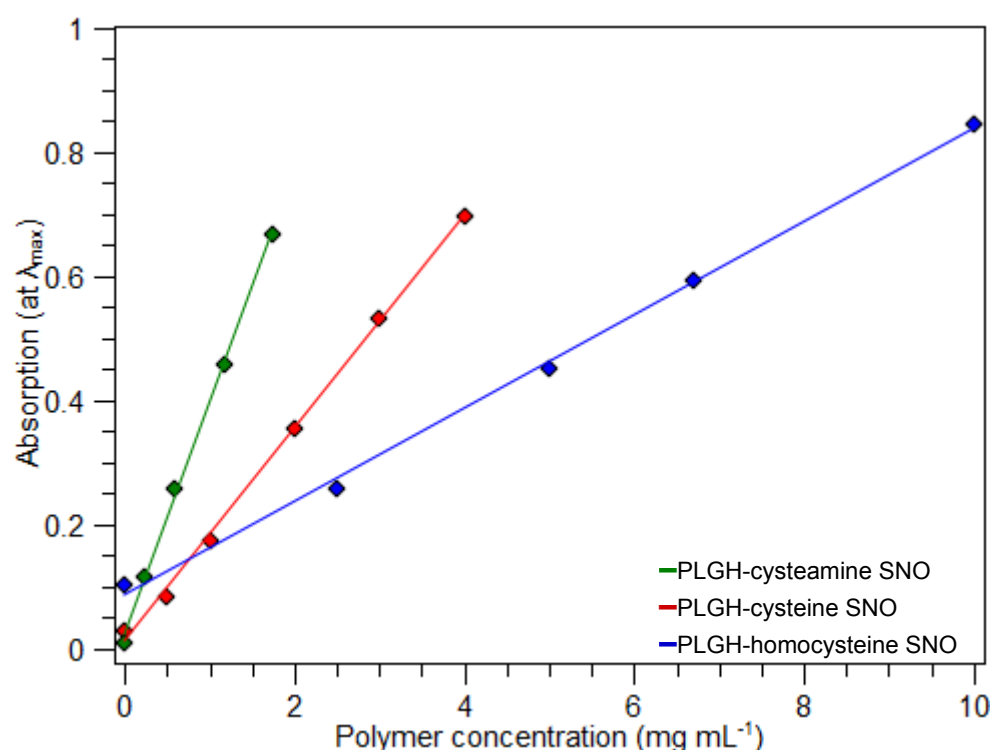
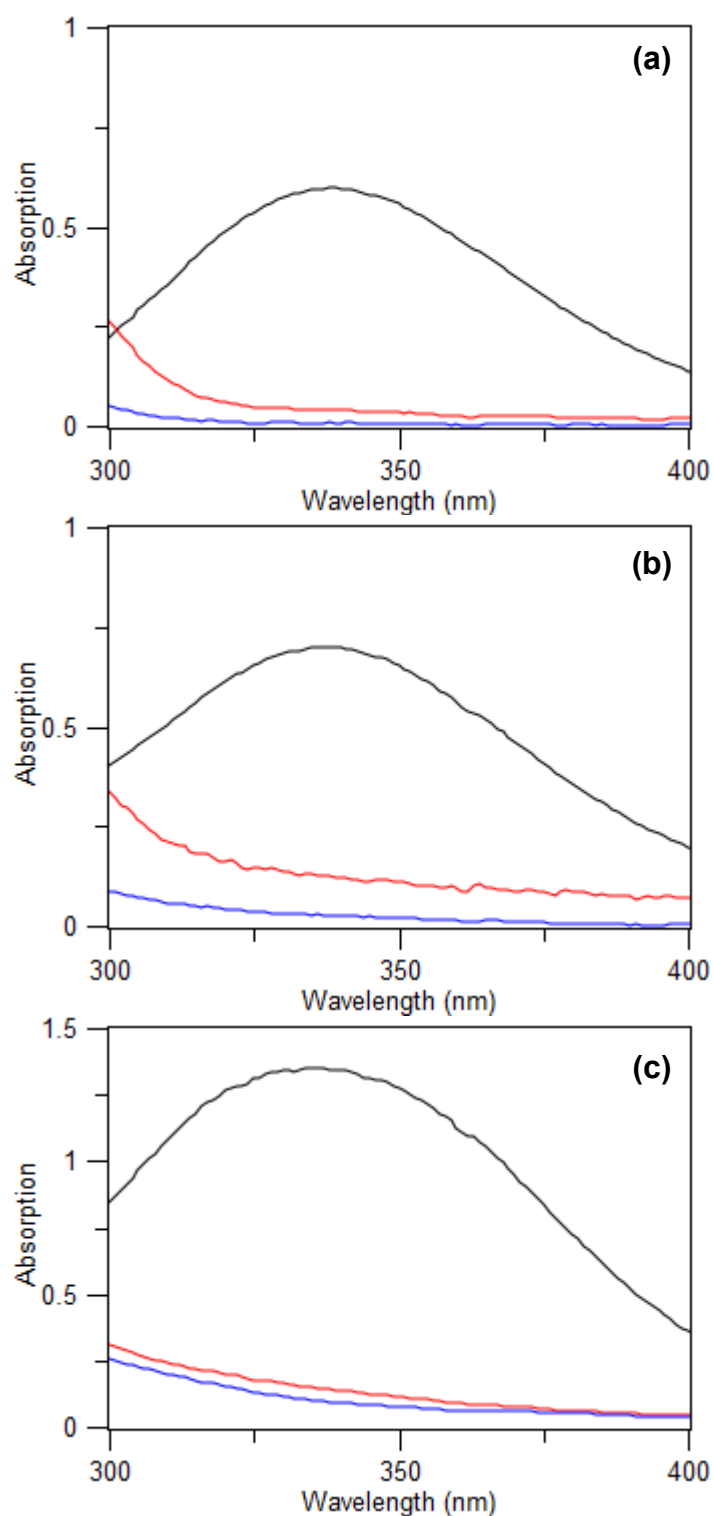


**Fig. S16** Absorption at 338 nm, 335 nm, and 336 nm as a function of polymer concentration for cysteamine (**2a**), cysteine (**2b**), and homocysteine (**2c**) PLGH derivatives, respectively. All calibration curves yielded an  $R^2 = 0.998$  and relative % error values of  $\leq 2\%$  associated with absorption values.

To determine a molar extinction coefficient value from the slope of the Beer's Law plot ( $A = \epsilon bc$  where  $b$  is a pathlength of 1 cm and  $c$  is the concentration of RSNO in mol L<sup>-1</sup>),

we converted the polymer concentration values ( $\text{mg mL}^{-1}$ ) into mol RSNO  $\text{L}^{-1}$ . This conversion involved the mol NO released per g material values that were collected via heat initiated decomposition NOA experiments for a single batch of each PLGH derivative.

It was necessary to determine the % RSNO decomposition that corresponded to the amount of NO recovered from each material (we cannot assume that our recovered NO corresponds to 100% of the NO reservoir within the material). To determine % RSNO decomposition, freshly *S*-nitrosated polymer solutions were prepared for UV absorption analysis at a concentration of 1.5, 4, and 20  $\text{mg mL}^{-1}$  for cysteamine (**2a**), cysteine (**2b**) and homocysteine (**2c**), respectively. After the NOA thermal decomposition analysis where samples were heated stepwise under dry conditions (37-100 °C temperature range), each material was recovered and dissolved to the same concentration as the freshly *S*-nitrosated sample. The absorption values at the  $\lambda_{\max}$  before and after RSNO decomposition determined the % RSNO decomposition. The absorption of a blank non-nitrosated sample was collected for each derivative (in the same concentration as the before and after NOA samples) and taken into consideration for the % RSNO decomposition determination (i.e. the blank sample represented 100% decomposition and the freshly *S*-nitrosated sample represented 0% decomposition and the sample after NOA analysis was determined accordingly). The absorption values for the non-nitrosated samples were taken to be the 0  $\text{mg mL}^{-1}$  points on the calibration curves (see Fig. S16). All absorption measurements and thermal NOA experiments were performed in triplicate with the error reported as the standard deviation. Fig. S17 shows representative UV spectra of each derivative before and after RSNO decomposition as well as the blank non-nitrosated sample, demonstrating that the RSNO moiety is decomposing to give rise to the detected NO.



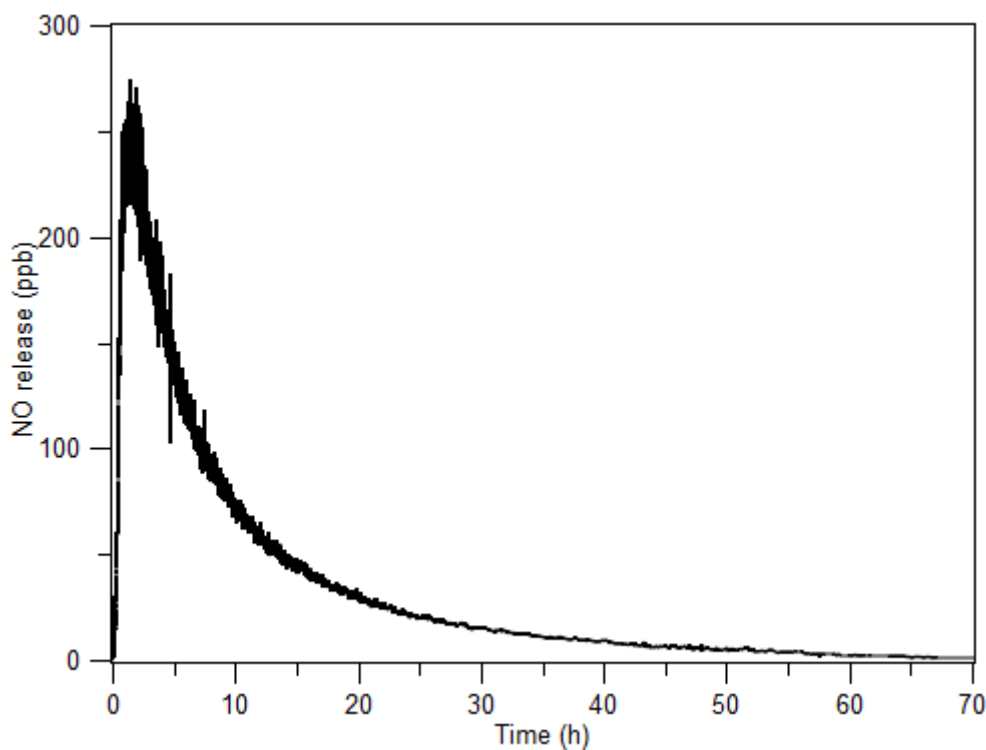
**Fig. S17** Representative absorption spectra for (a) cysteamine ( $1.5 \text{ mg mL}^{-1}$ ), (b) cysteine ( $4 \text{ mg mL}^{-1}$ ) and (c) homocysteine ( $20 \text{ mg mL}^{-1}$ ) PLGH derivatives dissolved in 2 methanol: 1 dichloromethane indicating freshly S-nitrosated samples (black), samples after NOA analysis (red) and non-nitrosated samples (blue).

Table S3 indicates the amount of NO recovered via thermal NOA analysis, the % decomposition determined from absorption analysis as well as the molar extinction coefficient value ( $\epsilon_{\max}$ ) that corresponds to the indicated  $\lambda_{\max}$  for each derivative. The error bars associated with the  $\epsilon_{\max}$  values were determined by performing a least-squares fit analysis to find the error in the slope.

**Table S3** NO recovery and absorption properties of various *S*-nitrosated PLGH derivatives.

Polymer	NO recovered ( $\times 10^{-4}$ mol g $^{-1}$ )	$\lambda_{\max}$ (nm)	% RSNO decomposition	$\epsilon_{\max}$ (M $^{-1}$ cm $^{-1}$ )
PLGH-cysteamine SNO ( <b>2a</b> )	4.61±0.36	338	94.9±2.5	766.0±19.7
PLGH-cysteine SNO ( <b>2b</b> )	1.68±0.19	335	86.2±0.2	882.9±18.2
PLGH-homocysteine SNO ( <b>2c</b> )	1.11±0.08	336	95.9±0.6	652.1±16.7

**S10. NO releasing kinetics**



**Fig. S18** A representative NO release profile of an *S*-nitrosated PLGH-cysteine (**2b**) polymer film presenting characteristic exponential decay over three days under physiological conditions.

**References**

1. V. B. Damodaran and M. M. Reynolds, *J. Mater. Chem.* 2011, **21**, 5870.